Vol 18 No 3, March 2009
1674-1056/2009/18(03)/1207-07

Chinese Physics B

© 2009 Chin. Phys. Soc.
and IOP Publishing Ltd

Structural, thermodynamic and electronic properties of zinc-blende AlN from first-principles calculations*

Zhang Wei(张 伟)[a], Cheng Yan(程 艳)[a], Zhu Jun(朱 俊)[a], and Chen Xiang-Rong(陈向荣)[a)b)†]

[a] *Institute of Atomic and Molecular Physics, Sichuan University, Chengdu* 610065, *China*

[b] *International Centre for Materials Physics, Chinese Academy of Sciences, Shenyang* 110016, *China*

(Received 1 September 2007; revised manuscript received 14 January 2008)

Structural, thermodynamic and electronic properties of zinc-blende AlN under pressure are investigated by first-principles calculations based on the plane-wave basis set. Through the analysis of enthalpy variation of AlN in the zinc-blende (ZB) and the rock-salt (RS) structures with pressure, we find the phase transition of AlN from ZB to RS structure occurs at 6.7 GPa. By using the quasi-harmonic Debye model, we obtain the heat capacity C_V, Debye temperature $\Theta_{\rm D}$, Grüneisen parameter γ and thermal expansion coefficient α. The electronic properties including fundamental energy gaps and hydrostatic deformation potentials are investigated and the dependence of energy gaps on pressure is analysed.

Keywords: local density approximation (LDA), thermodynamic properties, band structure, AlN
PACC: 7115M, 6740K, 7120H, 7155F

1. Introduction

Group-III nitride semiconductors have attracted much attention in recent years because of their great potential technological applications in optoelectronics areas.[1,2] Especially, aluminium nitride AlN is regarded as a promising wide bandgap semiconductor ranging from the ultraviolet (UV) to the visible light regions of the spectrum, and so it can become one of the best materials for constructing devices in the violet region.[3] In addition, AlN has a high melting point, a high thermal conductivity, and a large bulk modulus.[4,5] Owing to the reactivity of AlN, a high-purity source material and an oxygen-free environment are required to grow AlN crystals of good quality.

In an ambient condition, AlN is generally reported to be non-polymorphous and it crystallizes in the wurtzite (WZ) structure with space group $P6_3mc$ (C_{6v}^4).[6] It has a mixture of covalent and ionic tetrahedral bondings. However, AlN can also grow in the zinc blende (ZB) cubic structure with space group $F\bar{4}3m$ (T_d^5)[7,8] and NaCl-like rocksalt (RS) structure with space group $Fm\bar{3}_m$ (O_h^5).[9,10] The phase transitions of AlN under pressure especially from WZ structure to RS structure have been reported both theoretically and experimentally.[9,11,12] However, for the phase transition of AlN from the ZB structure to the RS structure, there are two opposite viewpoints. Serrano *et al* [13] and Goumri-Said *et al* [14] reported that the phase transition could occur, but Siegel *et al* [15] came to a completely different conclusion that there appeared neither WZ–ZB nor RS–ZB phase transition. Moreover, although several theoretical studies[12,16−18] have been carried out on the ZB structure AlN, the basic physical properties such as structural, thermodynamic and electronic structure properties are little known, especially for the ZB AlN under pressure.

The aim of this work is to give a comparative and complementary investigation on structural, thermodynamic and electronic properties of the ZB AlN under pressure by using the plane-wave pseudopotential density functional theory method and the Cambridge Serial Total Energy Package (CASTEP) program.[19,20] After a brief description of calculation details, we give a calculation of the ground state properties for both ZB AlN and RS AlN. Subsequently, a detailed investigation of various properties for AlN in ZB structure is conducted.

*Project supported by the National Natural Science Foundation of China (Grant No 10776022).
†Corresponding author. E-mail: xrchen@126.com

2. Theoretical framework

2.1. Total energy electronic structure calculations

In the electronic structure calculations, the ultrasoft pseudopotentials introduced by Vanderbilt[21] are employed for all the ion–electron interaction together with the local density approximation (LDA) proposed by Vosko *et al* [22] as an exchange-correlation function. A plane-wave basis set with an energy cut-off of 500 eV is applied. Pseudo-atomic calculations are performed for Al $3s^2 3p^1$ and N $2s^2 2p^3$. For the Brillouin zone sampling, in the calculation of ground state properties, we use a 6×6×6 Monkhorst–Pack mesh, however, in the band structure calculation we use a 12×12×12 Monkhorst–Pack mesh. The self-consistent convergence of the total energy is 10^{-6} eV/atom. All these total-energy electronic structure calculations are implemented by using the CASTEP code.[19,20]

2.2. Thermodynamic properties

The quasi-harmonic Debye model is adapted for the investigation of thermodynamic properties, in which the non-equilibrium Gibbs function G^* (V; P, T) can be written in the form of

$$G^*(V;P,T) = E(V) + PV + A_{\rm Vib}(\Theta(V);T), \quad (1)$$

where $E(V)$ is the total energy per unit cell for AlN, PV corresponds to the constant hydrostatic pressure condition, $\Theta(V)$ is the Debye temperature, and $A_{\rm vib}$ is the vibrational Helmholtz free energy that can be written as[23,24]

$$A_{\rm Vib}(\Theta;T) = nkT\left[\frac{9}{8}\frac{\Theta}{T} + 3\ln(1-{\rm e}^{-\Theta/T}) - D(\Theta/T)\right] \quad (2)$$

with $D(\Theta/T)$ representing the Debye integral, n denoting the number of atoms per formula unit. For an isotropic solid, Θ is expressed as

$$\Theta = \frac{\hbar}{k}\left[6\pi^2 V^{1/2} n\right]^{1/3} f(\sigma)\sqrt{\frac{B_{\rm S}}{M}}, \quad (3)$$

where M is the molecular mass, $B_{\rm S}$ is the adiabatic bulk modulus, which is approximated by the static compressibility as[25]

$$B_{\rm S} \cong B(V) = V\left\{\frac{{\rm d}^2 E(V)}{{\rm d}V^2}\right\}. \quad (4)$$

The Poisson σ is taken as 0.25. Therefore, the non-equilibrium Gibbs function G^* (V; P, T) as a function of (V; P, T) can be minimized with respect to volume V

$$\left(\frac{\partial G^*(V;P,T)}{\partial V}\right)_{P,T} = 0. \quad (5)$$

By solving Eq.(5), one can obtain the thermal equation of state, V (P, T). The heat capacity C_V and the thermal expansion coefficient α are given by[26]

$$B_T(P,T) = V\left(\left(\frac{\partial^2 G^*(V;P,T)}{\partial V^2}\right)_{P,T}\right), \quad (6)$$

$$C_V = 3nk\left[4D(\Theta/T) - \frac{3\Theta/T}{{\rm e}^{\Theta/T}-1}\right], \quad (7)$$

$$\alpha = \frac{\gamma C_V}{B_T V}, \quad (8)$$

where γ is the Grüneisen parameter, which is defined as

$$\gamma = -\frac{{\rm d}\ln\Theta(V)}{{\rm d}\ln V}. \quad (9)$$

Applying these methods described above, we have successfully investigated the thermodynamic properties of Li_2O,[27] BN[28] and AlB_2.[29]

3. Results and discussion

3.1. Structure and phase transition of AlN

For both the ZB structure and the RS structure of AlN, a series of values of lattice constant a is set to obtain the total energy E and the corresponding primitive cell volume V, and then the obtained $E-V$ data are fitted to the Birch–Murnaghan equation of state.[30] The obtained values of equilibrium lattice constant a, zero-pressure bulk modulus B_0 and its pressure derivative B_0' are summarized in Table 1. Moreover, the elastic constants of the ZB AlN at zero pressure are also listed there. All these results are consistent with other calculated results[12−18,31−36,37] and the available experimental data,[9,11,38] which implies the validity of the present calculation.

Table 1. Structural and elastic constants of the ZB structure AlN at $P = 0$ and $T = 0$.

	present work	other calculations	experiments
ZB structure			
a/nm	0.431	0.431–0.4376[a] 4.379[b]	0.437[c]
B_0/GPa	212.8	211–216[a] 224[b]	–
B_0'	3.735	3.2–3.86[a] 4.242[b]	–
C_{11}/GPa	301	304[d] 313[e] 313.24[f]	–
C_{12}/GPa	160	152[d] 160[e] 156.47[f]	–
C_{44}/GPa	202	199[d] 192[e] 202[f]	–
RS structure			
a/nm	0.3982	0.4229[b] 0.3978[g] 0.406[h]	0.4045[i]
B_0/GPa	280.7	297.6[b] 272[g]	295[j]
B_0'	3.914	3.05[b] 3.8[g]	3.5[j]

[a] Refs.[12,16–18,31–36]; [b]Ref.[14]; [c]Ref.[38]; [d] Ref.[17]; [e] Ref.[32]; [f]Ref.[37]; [g]Ref.[13]; [h]Ref.[15]; [i]Ref.[11]; [j]Ref.[9].

On the basis of these results, it should be interesting to study the structural properties of AlN under pressure. A theoretical estimate of the zero-temperature transition pressure between the ZB AlN and the RS AlN can be obtained from the usual condition of equal enthalpies, i.e. the pressure P, at which the values of enthalpy $H = E + PV$ of both phases are the same. Figure 1 shows the enthalpy variations of AlN in the ZB and the RS structures with pressure. It is found that the phase transition of AlN from the ZB structure to the RS structure occurs at 6.7 GPa, well consistent with the value 7.1 GPa calculated by Serrano *et al* from *ab initio* method,[13] but a little larger than 5 GPa given by Goumri-Said *et al*,[14] who performed their calculation by molecular dynamics simulation based on the Tersoff empirical interatomic potential.

3.2. Thermodynamic properties of the ZB AlN

The quasi-harmonic Debye model empowers us to obtain heat capacity C_V, Debye temperature $\Theta_{\rm D}$, Grüneisen parameter γ and thermal expansion coefficient α successfully. In Fig.2, we plot the dependence of heat capacity C_V on temperature at zero pressure together with the experimental data. A comparison between the calculated values and the experimental data available[4,39] reveals their excellent agreement for the entire temperature range. It can be found that when the temperature is below 600 K, the heat capacity C_V is strongly dependent on temperature, which is due to the anharmonic approximation used in the calculation. However, at higher temperatures, the anharmonic effect on C_V is suppressed. At zero

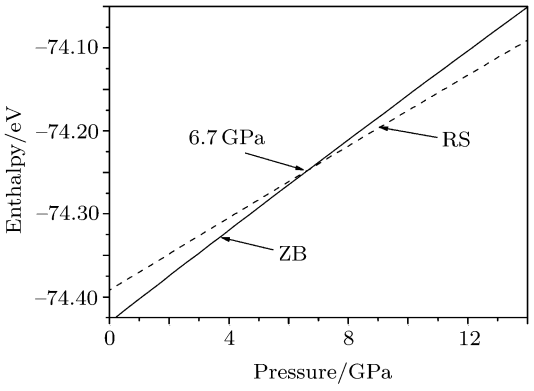


Fig.1. Plots for enthalpy versus pressure for ZB AlN and RS AlN.

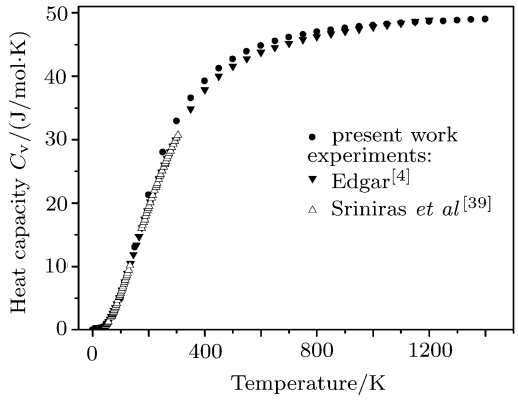


Fig.2. Comparison between the calculated heat capacity and the available measurements for ZB AlN.

pressure and ambient temperature, the heat capacity in the present work is 31.55 J/(mol·K) which is close to 29.95 J/(mol·K) given by Edgar[4] and 30.71 J/(mol·K) by Srinivas *et al.*[39] As temperature increases, the heat capacity approaches to the Dulong–Petit result (≈49.90 J/(mol·K)), which is followed by all solid circles at high temperatures.

Moreover, the variations of Debye temperature $\Theta_{\rm D}$, Grüneisen parameter γ and thermal expansion coefficient α with temperature at 0 and 6.7 GPa are illustrated in Figs.3(a)–3(c), respectively. At a constant pressure, both the Grüneisen parameter γ and the thermal expansion coefficient α increase with temperature increasing, however, the Debye temperature $\Theta_{\rm D}$ decreases with the increase of temperature. For a constant temperature, the values of Grüneisen parameter γ and thermal expansion coefficient α at 6.7 GPa are higher than those at 0 GPa, while Debye temperature $\Theta_{\rm D}$ at 6.7 GPa is lower than at 0 GPa. This can be understood from the fact that the effect of temperature on materials is contrary to that of pressure.

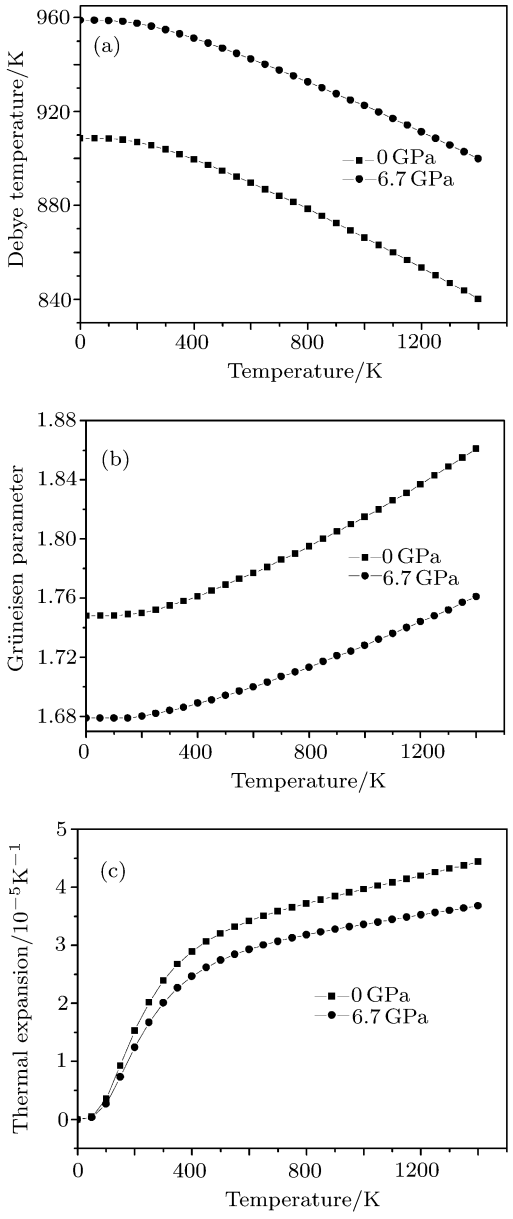


Fig.3. The temperature dependences of (a) Debye temperature $\Theta_{\rm D}$, (b) Grüneisen parameter γ, and (c) thermal expansion coefficient α of ZB AlN at pressures of 0 and 6.7 GPa.

We can also obtain the Debye temperature of the ZB AlN form the elastic constants by using the following empirical relation:[14]

$$\theta_D = -11.3964 + 0.3475 C_{11} - 1.6150 \times 10^{-5} C_{11}^2. \quad (10)$$

The calculated Debye temperature of the ZB AlN is 888.3 K, which is a little smaller than 908.6 K obtained from the quasi-harmonic Debye model. A comparison between 908.6 K obtained from the quasi-harmonic Debye model and 911.6 K given by Goumri–Said *et al*,[14] implies that the quasi-harmonic Debye model is superior to the empirical relation. In addition, using the following empirical relation:[40]

$$T_{\rm m} = 553{\rm K} + (591/10^{11}{\rm Pa}) C_{11} \pm 300{\rm K}, \quad (11)$$

we can also obtain the melting temperature of the ZB AlN. The melting temperature of the ZB AlN is 2332±300 K, which is smaller than 2800 K of the WZ AlN.[41] Because the elastic constant C_{11} increases with applied pressure, it may be reasonable to assume that the melting temperature of the ZB AlN will increase with pressure increasing.

3.3. Electronic properties of the ZB AlN under pressure

Band dispersions along high symmetry lines of the ZB AlN at zero pressure and transition pressures are given in Fig.4, where the top of the valence band is taken as zero energy. At normal pressure, it can be seen that the valence band maximum is at the Gamma (G) point and the conduction appears at X point. Therefore, the ZB AlN has an indirect band energy gap of 3.30 eV, which is smaller than 6.2 eV for its WZ structure[42] and 4.65 eV for RS structure.[12] The band gaps of $G_{\rm v} - G_x$ and $G_{\rm v} - L_{\rm c}$ together with the full valence band width (FVBW) and antisymmetric gap ($E_{\rm asy}$) are also obtained. Those results are all listed in Table 2 together with other calculations. It can be seen that our results at zero pressure accord with them very well.

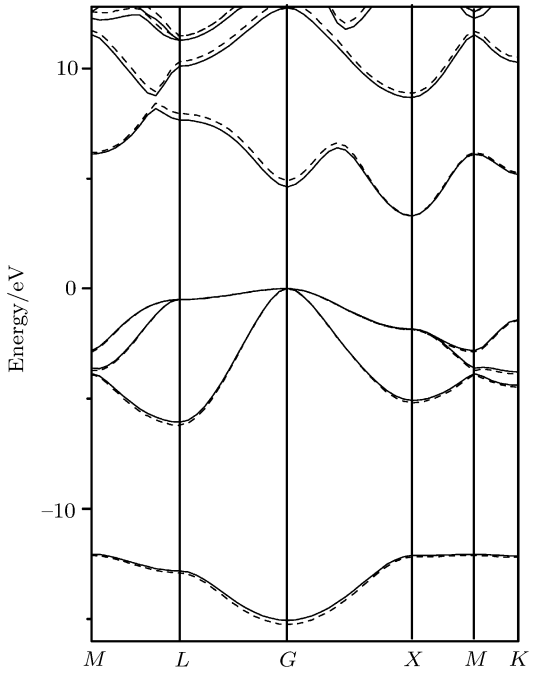


Fig.4. Band structures at pressures of 0 (solid) and 6.7 GPa (dashed) for ZB AlN.

Table 2. Calculated bandgaps (eV), antisymmetric gap ($E_{\rm asy}$) and FVBW of the ZB AlN.

energy gaps	present work	other calculations			
$G_{\rm v}-G_{\rm c}$	4.63	4.58[a]	4.52[b]	4.3[c]	4.75[d]
$G_{\rm v}-X_{\rm c}$	3.30	3.40[a]	3.36[b]	3.1[c]	3.2[e]
$G_{\rm v}-L_{\rm c}$	7.66	7.69[a]	7.65[b]	7.383[f]	
FVBW	15.06	14.92[f]	15.1[g]		
$E_{\rm asy}$	7.05	7.07[f]	7.6[g]		

[a]Ref.[12]; [b]Ref.[43]; [c]Ref.[44]; [d]Ref.[36]; [e]Ref.[31]; [f]Ref.[37]; [g]Ref.[45].

The applying of pressure can affect the electronic band structure of AlN. All the relative positions of the valence bands are shifted downwards while the conduction band is shifted downwards, however, the first conduction band at the X point is almost constant under the applied pressure, which indicates that the material of interest remains an indirect band gap ($G_{\rm v}\rightarrow X_{\rm c}$) semiconductor at the pressure studied. In addition, the full valence width increases from 15.06 to 15.24 eV as pressure increases from 0 to 6.7 GPa. Generally, as pressure increases, the lattice constant decreases, and so the valence band width increases. This trend can be ascribed to a reduction of hybridization with the increase of separation between atomic constituents. And it should be noted as well that the antisymmetric gap is affected by pressure, thereby leading to a slight reduction of this gap, from 7.05 to 7.00 eV.

In order to perform a further study of the effect of pressure on the electronic structure of the ZB AlN, the band energies at selected symmetry points are examined as a function of pressure, of which the results are shown in Fig.5(a). It is noted that the direct gap and the indirect gap $G_{\rm v}-G_{\rm c}$, $G_{\rm v}-L_{\rm c}$ and $G_{\rm v}-X_{\rm c}$ increase almost linearly as pressure increases. Moreover, the change in energy band gap is often presented against the ratio $\Delta a/a_0$ where $\Delta a=a_{\rm P}-a_0$, $a_{\rm P}$ and a_0 are the lattice constants at pressure P and at zero pressure, respectively. The dependences of direct and indirect band gaps, namely $G_{\rm v}-G_x$, $G_{\rm v}-X_{\rm c}$ and $G_{\rm v}-L_{\rm c}$, on $\Delta a/a_0$ are plotted in Fig.5(b). The solid lines represent the results of least-square fitting to the data, obtained by using the quadratic fitting. It can be found that the behaviour of the energy band gaps against $\Delta a/a_{\rm T}$ is non-linear which is qualitatively similar to those of other III–V semiconductor compounds.[12]

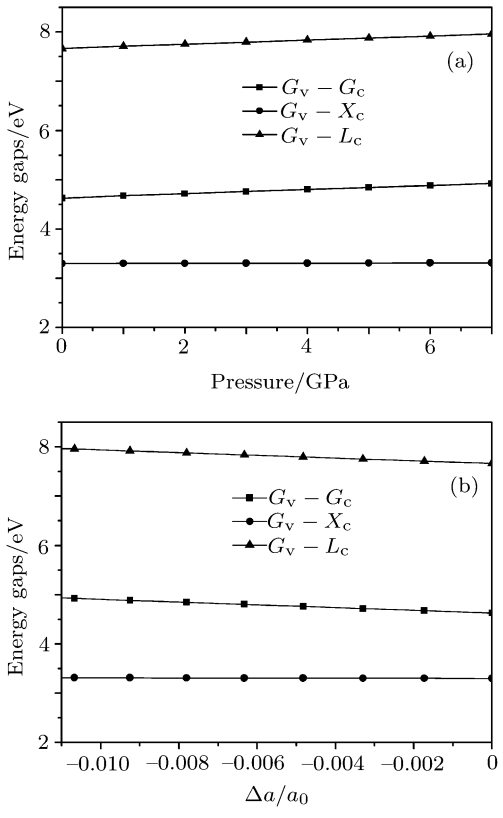


Fig.5. (a) Direct and indirect bandgap energies versus pressure of ZB AlN, and (b) calculated dependences of the direct and indirect bandgaps of ZB AlN on lattice constant.

The deformation potentials, which are important parameters for describing electronic effects originating from strains, are obtained by using the following

expression:

$$\alpha_{\mathrm{g}} = V\frac{\mathrm{d}E_{\mathrm{g}}}{\mathrm{d}V}. \tag{12}$$

The application of hydrostatic pressure empowers us to directly estimate the hydrostatic deformation potential for the bandgap of ZB AlN. Such a calculation is required for an interface calculation between compressed and expanded regions of the crystal to determine their band lineup; therefore, they depend on crystal orientation. To our knowledge, no experimental data for the hydrostatic deformation potential are presently available for AlN in ZB structure, so in the present work, the deformation potentials for the energy gaps at the points of high symmetry are calculated and listed in Table 3, together with other theoretical calculations for comparison. It can be found that our results consist with them very well.

Table 3. Calculations of deformation potential constant α_{g} (in eV) for ZB AlN.

α_{g}/eV	present work	other calculations		
$G_{\mathrm{v}} - G_{\mathrm{c}}$	–9.268	–9.0[a]	–9.26[b]	–9.26[c]
$G_{\mathrm{v}} - X_{\mathrm{c}}$	–0.468	–0.37[a]	–0.42[b]	–0.436[c]
$G_{\mathrm{v}} - L_{\mathrm{c}}$	–9.232	–9.4[a]	–9.04[b]	–9.35[c]

[a] Ref.[12]; [b]Ref.[46]; [c]Ref.[37].

4. Conclusion

We have performed a detailed investigation on structural, thermodynamic and electronic properties of the ZB AlN under pressure. The ZB–RS phase transition is found to occur at a pressure of 6.7 GPa. By using the quasi-harmonic Debye model, we have also obtained heat capacity C_V, Debye temperature Θ_{D}, Grüneisen parameter γ and thermal expansion coefficient α. Within the LDA approximation, an indirect gap of 3.30 eV induced by the transition from G_{v} to X_{c} is calculated, which together with hydrostatic deformation potential constants provides an excellent description of the stress effects on band structures of AlN.

References

[1] Wu Y F, Keller B P, Keller S, Kapolnek D, Kozodoy P, Denbaars S P and Mishra U K 1996 *Appl. Phys. Lett.* **69** 1438

[2] Liu F S, Liu Q L, Liang J K, Luo J, Su J, Zhang Y, Sun B J and Rao G H 2006 *Chin. Phys.* **15** 2445

[3] Jonnard P, Capron N, Semond F, Massies J, Martinez-Guerrero E and Mariette H 2004 *Euro. Phys. J.* B **42** 351

[4] Edgar J H 1994 *Properties of Group III Nitrides Electronic Materials Information Service (EMIS) Data Reviews Series* (London: Institution of Electrical Engineers)

[5] Ponce F A and Bour D P 1997 *Nature* **386** 351

[6] Nakamura S, Senoh M, Nagahama S, Iwasa N, Yamada T, Matsushita T, Sugimoto Y and Kikoyu H 1997 *Jpn. J. Appl. Phys.* **36** 1059

[7] Petrov I, Mojab E, Powell R C, Greene J E, Hultman L and Sundgren J E 1992 *Appl. Phys. Lett.* **60** 1491

[8] Thompson M P, Auner G W, Zheleva T S, Jones K A, Simko S J and Hilfiker J N 2001 *J. Appl. Phys.* **89** 3331

[9] Xia Q, Xia H and Ruoff A L 1993 *J. Appl. Phys.* **73** 8193

[10] Xia Q, Xia H and Ruoff A L 1993 *J. Appl. Phys.* **73** 12925

[11] Uehara S, Masamoto T, Onodera A, Ueno M, Shimomura O and Takemura K 1997 *J. Phys. Chem. Solids* **58** 2093

[12] Christensen N E and Gorczyca I 1994 *Phys. Rev.* B **50** 4397

[13] Serrano J, Rubio A, Hernández E, Munoz A and Mujica A 2000 *Phys. Rev.* B **62** 16612

[14] Goumri-Said S, Kanoun M B, Merad A E, Merad G B and Aourag H 2004 *Chem. Phys.* **302** 135

[15] Siegel A, Parlinski K and Wdowik U D 2006 *Phys. Rev.* B **74** 104116

[16] Wright A F 1997 *J. Appl. Phys.* **82** 2833

[17] Kim K, Lambrecht W R L and Segall B 1996 *Phys. Rev.* B **53** 16310

[18] Karch K, Wagner J M and Bechstedt F 1998 *Phys. Rev.* B **57** 7043

[19] Payne M C, Teter M P, Allen D C, Arias T A and Joannopoulos J D 1992 *Rev. Mod. Phys.* **64** 1045

[20] Milman V, Winkler B, White J A, Packard C J, Payne M C, Akhmatskaya E V and Nobes R H 2000 *Int. J. Quantum Chem.* **77** 895

[21] Vanderbilt D 1990 *Phys. Rev.* B **41** 7892

[22] Vosko S H, Wilk L and Nusair M 1980 *Can. J. Phys.* **58** 2100

[23] Blanco M A, Mart´in P A, Francisco E, Recio J M and Franco R 1996 *J. Mol. Struct.* (Theochem.) **368** 245

[24] Flórez M, Recio J M, Francisco E, Blanco M A and Pendás A M 2002 *Phys. Rev.* B **66** 144112

[25] Pugh S K, Dugdale D J, Brand S and Abram R A 1999 *Semicond. Sci. Technol.* **14** 23

[26] Francisco E, Blanco M A and Sanjurjo G 2001 *Phys. Rev.* B **63** 094107

[27] Li X F, Chen X R, Meng C M and Ji G F 2006 *Solid State Commun.* **139** 197

[28] Hao Y J, Cheng Y, Wang Y J and Chen X R 2007 *Chin. Phys.* **16** 217

[29] Zhou X L, Liu K, Chen X R and Zhu J 2006 *Chin. Phys.* **15** 3014

[30] Birch F 1947 *Phys. Rev.* **71** 809

[31] Vogel D, Kruüger P and Pollmann J 1997 *Phys. Rev.* B **55** 12836

[32] Shimada K, Sota T and Suzuki K 1998 *J. Appl. Phys.* **84** 4951

[33] Bechstedt F, Grossner U and Furthmüller J 2000 *Phys. Rev.* B **62** 8003

[34] Zoroddu A, Bernardini F, Ruggerone P and Fiorentini V 2001 *Phys. Rev.* B **64** 045208

[35] Fuchs M, Da Silva J L F, Stampfl C, Neugebeaur J and Scheffler M 2002 *Phys. Rev.* B **65** 245212

[36] Stampfl C and van de Walle C G 1999 *Phys. Rev.* B **59** 5521

[37] Kanoun M B, Goumri-Said S, Merad A E, Merad G, Cibert J and Aourag H 2004 *Semicond. Sci. Technol.* **19** 1220

[38] Trampert A, Brandt O, Ploog K H in: 1998 Pankove J I, Moustakas T D (eds) *Crystal Structure of Group III Nitrides, Semiconductors and Semimetals* **50** (San Diego: Academic)

[39] Srinivas R, Sulze D and Schwarz H 1990 *J. Am. Chem. Soc.* **112** 8334

[40] Fine M E, Brown L D and Marcus H L 1984 *Scr. Metall.* **18** 951

[41] Massalski T B 1990 *Binary Alloys, Phase Diagrams* Second edition (USA: ASM International) p176

[42] Madelung O, Blachnik R and Kress W in: 1982 Semiconductors Madelung O, Schulz M and Weiss H (eds) *LandoltBörnstein, New Series* Group III Vol. **III** Part 17a (Berlin: Springer-Verlag)

[43] van Camp P E, van Doren V F and Devreese J T 1992 *Phys. Rev.* B **44** 9056
van Camp P E, van Doren V F and Devreese J T 1992 *Solid State Commun.* **81** 23

[44] Pugh S K, Dugdale D J, Brand S and Abram R A 1999 *Semicond. Sci. Technol.* **14** 23

[45] Rubio A, Corkill J L, Cohen M L, Shirley E L and Louie S G 1993 *Phys. Rev.* B **48** 11810

[46] Wei S H and Zunger A 1999 *Phys. Rev.* B **60** 5404